Original research paper (Oryginalny artykuł naukowy)

mgr inż. Julia Blazy[1)*)]
ORCID: 0000-0001-9525-8650
prof. dr hab. inż. Łukasz Drobiec[1)]
ORCID: 0000-0001-9825-6343

The application of flexural test results in the design of FRC ground slabs

Zastosowanie wyników badań na zginanie w projektowaniu fibrobetonowych posadzek na gruncie

DOI: 10.15199/33.2024.01.02

Abstract. The article presents the results of testing three polymer fiber reinforced concretes (FRC). The influence of fiber type and dosage became evident after cracking of beams. Based on the calculated equivalent and residual flexural tensile strengths, fracture energy, and toughness index, it was stated that FRC with the highest amount of macrofibers achieved the best results. The third and fourth editions of Technical Report 34 were compared and it was claimed that the fiber addition enables an increase in the load – carrying capacity of the ground slabs loaded at the centre and on the edge.
Keywords: fiber reinforced concrete; polymer fibers; four – point bending test; ground slab.

Streszczenie. Artykuł przedstawia wyniki badań trzech fibrobetonów z dodatkiem włókien polimerowych. Wpływ rodzaju i ilości włókien był widoczny po zarysowaniu się belek. Na podstawie obliczonych wytrzymałości równoważnych, resztkowych, energii pękania oraz ilorazów odporności na pękanie stwierdzono, że fibrobeton z największą ilością makrowłókien osiągał najlepsze wyniki. Porównano trzecią i czwartą edycję Raportu Technicznego 34 oraz uznano, iż dodatek włókien umożliwia zwiększenie nośności płyty na gruncie obciążonej w środku oraz na krawędzi.
Słowa kluczowe: fibrobeton; włókna polimerowe; test czteropunktowego zginania; posadzka na gruncie.

Fiber reinforced concrete (FRC) is increasingly used in construction and architecture due to its improved strength, durability and ability to bridge cracks [1]. However, the scope of its applications is still quite limited, as despite a large number of tests on small--scale specimens, there are few tests on large-scale models. In addition, there is a lack of clear procedures for the design of FRC elements, especially with non-metallic fibers. One publication that provides guidelines for the design of FRC industrial floors is Technical Report 34 (TR34). It takes into account the possibility of using residual load-bearing capacities resulting from the addition of fibers to concrete. The calculation procedure for permissible concentrated loads acting on the slab on the ground uses Meyerhof's theory. According to the third edition of TR34 [2], it was required to determine the value of R_e (fracture toughness index) based on the four-point bending test (4PBT). In contrast, the current fourth edition of TR34 [3] uses $f_{R,j}$ (residual flexural tensile strength) values obtained from a three-point bending test (3PBT). The purpose of the article was to compare the two editions, since older technical sheets of fibers and projects still operate with R_e values, while newer ones already operate with $f_{R,j}$ values. The comparison was made based on the results of the 3PBT, described in detail in [4], and the results of the 4PBT of the three FRC with the addition of polymer fibers, presented in this article.

Research program

As part of the research program, three FRC (no. 1 – 3) were made with the addition of micro and macro polymer fibers (microPF and macroPF), differing in type (Table 1) and dosage. In the mixture design cement CEM II/A-V 42.5R was used, moreover metakaolin (MK) was added, and due to the expected deterioration in workability resulting from the addition of fibers, superplasticizer (SP) was also applied (Table 2). A detailed description of the materials and fibers used can be found in [4, 5]. Three 150 x 150 x 700 mm beams were made from each FRC mix for the 4PBT. The 4PBT was conducted 112 days after concreting according to the EN 12390-5 [6] and JCI-SF4 [7] on the testing set-up shown in the photograph. Displacement sensors (LVDTs) were installed on two sides of the specimen to measure beam deflection (δ). The span between supports (l) was 450 mm. The beams were loaded with a force (F) that increased with deflection (0.2 mm/min) until δ = 5 mm was reached. During the 4PBT, the F – δ graph was recorded. Using the formula in [6], it was converted to a graph of $f_{cf} – \delta$ and the maximum flexural tensile strength $f_{cf,max}$ was determined.

Table 1. Characteristics of polymer fibers
Tabela 1. Charakterystyka włókien polimerowych

Property/Type	I – macroPF	II – macroPF	III – microPF
Length [mm]	42	54	12
Tensile strength [MPa]	550	640	350 – 400
Young modulus [GPa]	2,8 – 4,0	11	unknown

[1)] Faculty of Civil Engineering, Silesian University of Technology
[*)] Correspondence address:julia.blazy@polsl.pl

Table 2. FRC mixture composition [kg/m³]
Tabela 2. Skład mieszanek fibrobetonowych [kg/m³]

FRC/Composition	Cement	Sand	Gravel	Water	SP	MK	PF (type I + II + III)
no. 1	350	800	1050	185	4,6	25	2 + 0 + 1
no. 2	350	800	1050	185	4,6	25	0 + 2 +1
no. 3	350	800	1050	185	4,2	25	0 + 2,5 + 0,5

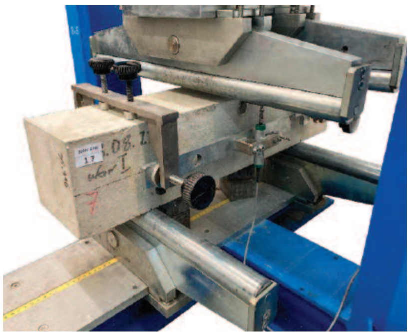

Testing set-up for 4PBT
Stanowisko badawcze do testu 4PBT

Research results

Figure 1 shows the $f_{cf} - \delta$ graphs, where in the description of samples X.Y_4PBT, X stands for the number of the mixture (1 – 3) and Y for the number of the tested beam (7 – 9, no. 1 – 6 were tested in the 3PBT [4]). The similar behavior of the FRC samples in the 4PBT and 3PBT confirmed the correctness of the tests conducted. Namely, FRC no. 1 and no. 2 were characterized by a very similar course of the $f_{cf} - \delta$ graph. This was due to the same content of macroPF and microPF (2 and 1 kg/m³, respectively). However, when δ = 1 mm was reached, FRC no. 2 achieved slightly higher strengths, which was due to the greater length and tensile strength of the fibers added to this mix (Type II) compared to the fibers used in no. 1 (Type I). Both FRC no. 1 and 2 represented a material with softening behavior. In contrast, the increased amount of macroPF in no. 3 (2.5 kg/m³) leaded to the highest strength values and was characterized by soft – hardening behavior. Figure 2 shows the $f_{cf,max}$ values determined in accordance with EN 12390-5 [6] for the 4PBT, along with their comparison with $f^{f}_{ct,L}$, the maximum flexural tensile strength determined in the 3PBT. It can be concluded that in the 4PBT, FRC no. 3 achieved the highest $f_{cf,max}$ value: 7 and 13% higher than no. 1 and no. 2, respectively. The average value of $f_{cf,max}$ for all mixes was 3.723 MPa. Comparing the results of the maximum strengths from the 3PBT and 4PBT, the differences range from 1 to 9% (Figure 2). All beams in the 4PBT were damaged by a quasi-vertical crack occurring between the upper supports. At the end of the test, the beams did not break in half, but retained their integrity. On the other hand, the abrupt drops in the graphs in Figure 1 in the post-cracking phase were indicative of pullout or breakage of the fibers in the cross-section of the crack.

Fig. 2. Maximum flexural tensile strength from 3PBT and 4PBT
Rys. 2. Maksymalna wytrzymałość na rozciąganie przy zginaniu w testach 3PBT i 4PBT

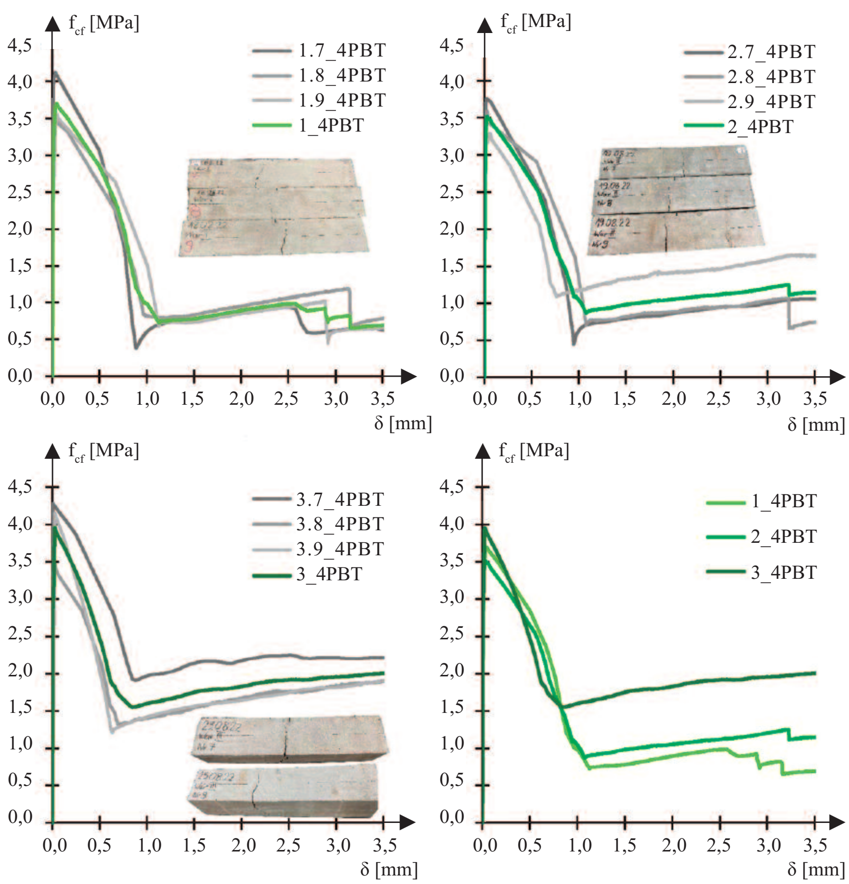

Fig. 1. $f_{cf} - \delta$ dependency obtained from 4PBT
Rys. 1. Zależność $f_{cf} - \delta$ uzyskana z testów 4PBT

The 4PBT methodology, in terms of specimen geometry, location of supports and loading, meets the requirements of JCI-SF4 [7]. Thus, the equivalent flexural tensile strength f_{eq} was calculated using equation (1). However, it is necessary to know the value of T_b, i.e. the work required to obtain δ of the beam equal to $^{1}/_{150}$ of its span. This work was calculated as the area under the F – δ averaged for each no. of FRC up to δ = 3 mm (Figure 3).

$$f_{eq} = \frac{T_b l}{\delta_{tb} b h^2} \tag{1}$$

where:

f_{eq} – equivalent flexural tensile strength [N/mm²];
T_b – work required to obtain δ of the beam equal to $^{1}/_{150}$ of the span l [Nmm];
l – span between bottom supports [mm] = 450 mm;
δ_{tb} – deflection equal to $^{1}/_{150}$ of the span l [mm] = 3 mm;
b, h – beam width and height [mm] = 150 mm.

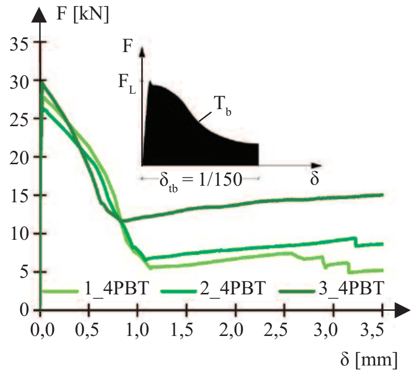

Fig. 3. F – δ plots obtained from 4PBT together with the calculation method of T_b
Rys. 3. Wykresy F – δ z testów 4PBT wraz ze sposobem obliczania T_b

Calculations show that FRC no. 1 is characterized by the smallest f_{eq}, while for no. 2 and no. 3 values that were respectively 5 and 42% higher were obtained (Table 3). Similar values were established in Glinicki's study [8]: f_{eq} was 1.30 and 1.87 MPa for samples with 2 and 3 kg/m^3 of synthetic macrofibers. By comparing the f_{eq} values with the residual ($f_{R,4}$) and equivalent ($f_{eq,3}$) strengths calculated in [4] in 3PBT according to standards [9] and [10], it is found that these values are not equal (Table 3), and therefore the relationships between them were determined (Figure 4a). Table 3 also summarizes the results of fracture energy W_0 calculations from 3PBT [4]. The method of calculating W_0 is shown in Figure 5. As in the 4PBT, the highest fracture energy was obtained by FRC no. 3, followed by no. 2 and finally no. 1 (Table 3). For fracture energy, the relationship between the 3PBT and 4PBT is also shown (Figure 4b). It should also be highlighted that f_{eq} strength is used to determine the fracture toughness index R_e (equation (2)). This index is used in the design of industrial floors in the third edition of TR34 [2] to take into account the residual load-bearing capacity due to the addition of fibers to the concrete mix. This effect is taken into account when calculating the positive bending moment M_p (equation (3)), provided that $R_e \geq 30\%$. In the calculations of R_e, as the value of $f_{ctm,fl}$, the experimentally determined value of $f_{cf,max}$ from 4PBT was taken. The values of R_e were equal 39%, 43% and 52% for FRC no. 1, 2 and 3, respectively. Thus, the most favorable results from the point of view of the element's load-bearing capacity would have been achieved if FRC no. 3 had been used. Nevertheless, the latest, fourth edition of TR34 [3] suggests conducting the 3PBT and, instead of the R_e, calculating the stresses σ_{r1} and σ_{r4}, equal to $0.45f_{R,1}$ and $0.37f_{R,4}$, respectively (equation (4)). In order to compare the two editions, the coefficients $TR34_3$ (3rd edition) and $TR34_4$ (4th edition) were calculated. The values of f_{eq} and $f_{R,4}$ are given in Table 3, while the values of $f_{R,1}$ were equal 1.979; 1.954 and 1.571 MPa for FRC no. 1, 2 and 3, respectively. From Figure 6, it can be concluded that M_p would be about 8 to 20% lower according to the fourth edition calculations.

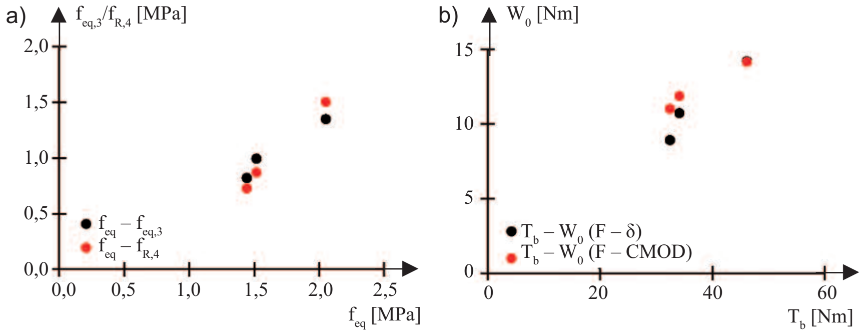

Fig. 4. Dependency between: a) $f_{eq} – f_{eq,3}$ and $f_{eq} – f_{R,4}$; b) $T_b – W_0$
Rys. 4. Zależność między: a) $f_{eq} – f_{eq,3}$ oraz $f_{eq} – f_{R,4}$; b) $T_b – W_0$

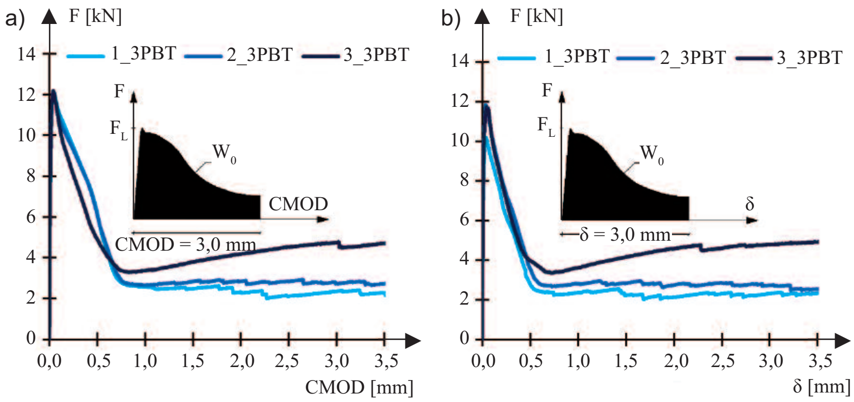

Fig. 5. Plots obtained from 3PBT tests together with the method of determining W_0 from the plot: a) F – CMOD; b) F – δ
Rys. 5. Wykresy uzyskane z testów 3PBT wraz ze sposobem określania W_0 z wykresu: a) F – CMOD; b) F – δ

$$R_e = 100 \cdot \frac{f_{eq}}{f_{ctm,fl}} \qquad (2)$$

where:
R_e – fracture toughness index [%];
f_{eq} – equivalent flexural tensile strength [N/mm^2];
$f_{ctm,fl}$ – mean flexural tensile strength [N/mm^2].

$$M_p = \frac{f_{ctk,fl}}{\gamma_c} \cdot R_e \cdot \frac{h^2}{6} = \frac{h^2}{\gamma_c} \cdot \frac{f_{eq}}{6} = \frac{h^2}{\gamma_c} \cdot TR34_3 \qquad (3)$$

$$M_p = (h^2/\gamma_c) \cdot (0{,}29\sigma_{r4} + 0{,}16\sigma_{r1}) = (h^2/\gamma_c) \cdot (0{,}29 \cdot 0{,}37f_{R,4} + 0{,}16 \cdot 0{,}45f_{R,1}) = (h^2/\gamma_c) \cdot TR34_4 \qquad (4)$$

where:
M_p – positive bending moment [Nm/m];
$f_{ctk,fl}$ – characteristics flexural tensile strength [N/mm^2];
γ_c – partial safety factor for materials [-] for FRC = 1,5;
h – slab thickness [mm];
σ_{r1} i σ_{r4} – stresses at the characteristic points corresponding to $f_{R,1}$ and $f_{R,4}$ [N/mm^2];
$f_{R,1}$ i $f_{R,4}$ – residua flexural tensile strength corresponding to CMOD = 0,5 and 3,5 mm [N/mm^2].

Table 3. Residual, equivalent strength and fracture energy from 3PBT and 4PBT
Tabela 3. Wytrzymałość resztkowa, równoważna i energia pękania w testach 3PBT i 4PBT

FRC no.	T_b [Nm]	f_{eq} [MPa]	$f_{eq,3}$ [MPa]	$f_{R,4}$ [MPa]	W_0 (F – δ) [Nm]	W_0 (F – CMOD) [Nm]
1	32,457	1,443	0,819	0,726	8,918	10,990
2	34,144	1,518	0,993	0,870	10,726	11,861
3	46,169	2,052	1,350	1,506	14,190	14,144

 ISSN 0137-2971, e-ISSN 2449-951X www.materialybudowlane.info.pl

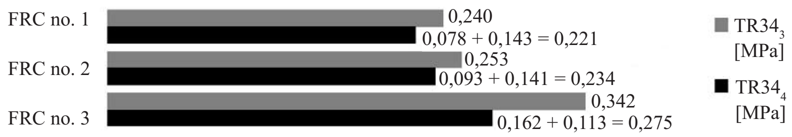

Fig. 6. Results of M_p according to [2, 3]
Rys. 6. Wyniki obliczeń M_p wg [2, 3]

The linear relationship proposed in Figure 7 links the results obtained for TR34 editions. However, further research must be done to confirm this correlation. The comparison of the TR34 editions is intended to enable the design of FRC structures regardless of which technical sheets and projects designers will be confronted with: the older ones based on R_e and the 3rd edition of TR34 or the newer ones with the given $f_{R,j}$ values required in the 4th edition of TR34. Bearing in mind that the 4th edition is applicable, the correlation will enable them to recalculate the data given in older fiber manufacturers' materials.

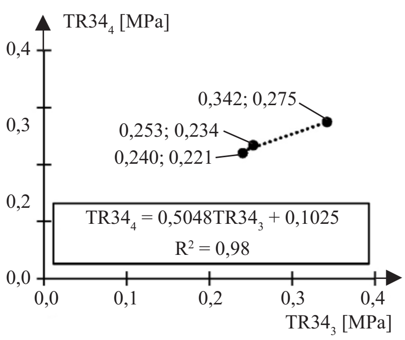

Fig. 7. Dependency between TR34$_3$ – TR34$_4$
Rys. 7. Zależność między TR34$_3$ – TR34$_4$

Finally, the effect of the fiber addition on the permissible point loads acting on the industrial floor was checked. The computational analyses were performed in accordance with the currently valid fourth edition of TR34. The procedures contained therein are based on Meyerhof's theory and take into account the bending capacity of the slab. Within the scope of the article, analyses related to the punching shear capacity of the slab were not carried out. For the calculations, a 150-mm-thick slab was assumed to be made of FRC no. 1, 2 and 3 from a concrete class C30/37. The maximum flexural tensile strength was taken as the averaged value from the 3PBT for all the tested beams, equal to 3.876 MPa [4]. Calculated values of residual flexural tensile strengths $f_{R,1}$ and $f_{R,4}$ were assumed for the FRC, while for the slab without fibers both values were assumed to be 0 MPa. The subgrade reaction modulus E_{v2} was assumed equal to 80 MPa (corresponding to a well-compacted sand). It was also assumed that the baseplate that transmits the point load to the slab has a diameter of 150 mm and a thickness of 20 mm. The assumed partial safety factors for concrete and FRC were equal 1.0 to calculate the characteristic values. It can be seen from Table 4 that the addition of polymer fibers has a beneficial effect on the flexural capacity of the slab loaded at the center and edge. In the calculation procedure for the corner, the effect of the fibers is not taken into account, hence no increase in allowable loads is noted. The resulting increase in load-bearing capacity at the center and edge of the slab is 34 – 43% and 15 – 19%, respectively, depending on the FRC used, compared to a slab without fibers.

Table 4. Permissible point loads acting on the ground slab according to [3]
Tabela 4. Dopuszczalne obciążenia punktowe działające na płytę na gruncie wg [3]

FRC no.	Slab center [kN]	Slab edge [kN]	Slab corner [kN]
without fibers	195 (100%)	119 (100%)	72 (100%)
1	262 (134%)	137 (115%)	72 (100%)
2	266 (136%)	138 (116%)	72 (100%)
3	278 (143%)	142 (119%)	72 (100%)

Conclusions

This paper presents the results of 4PBT of three FRC with the addition of polymer fibers. The results of maximum flexural tensile strengths from the 3PBT and 4PBT differed from 1 to 9%. The effect of the type and amount of fibers was evident after the beams were cracked, as only then fibers begin to bridge cracks. FRC no. 1 and no. 2 were characterized by similar strength values until δ equal to 1 mm. Then, due to higher tensile strength and length of used macrofibers, no. 2 reached slightly higher values. The best behavior was noted for FRC no. 3 due to the highest content of macrofibers. Similar conclusions were drawn from analyses of fracture energy and fracture toughness index. In addition, the third and fourth edition of TR34 were compared. The comparison was made to help designers of FRC structures, since the older technical sheets of fibers still operate with R_e values (4PBT) used in the 3rd edition of TR34, while the newer ones already operate with $f_{R,j}$ values (3PBT) according to the 4th edition of TR34. As a result of calculations of permissible point loads acting on the slab, it was found that the addition of fibers allows for an increase in the load-bearing capacity of the slab on the ground loaded at the center and at the edge.

Literatura

[1] A. Mohajerani i in. Amazing types, properties, and applications of fibres in construction materials. Materials. 2019; t. 12, nr 16, s. 2513. DOI: 10.3390/ma12162513.

[2] The Concrete Society, Technical Report 34. Concrete industrial ground floors. A guide to design and construction, 3. wyd. The Concrete Society, 2003.

[3] The Concrete Society, Technical Report 34. Concrete industrial ground floors. A guide to design and construction, 4. wyd. The Concrete Society, 2016.

[4] Drobiec Ł, Blazy J. Właściwości fibrobetonu określane w badaniach normowych – test wytrzymałości na ściskanie oraz test trzypunktowego zginania. Materiały Budowlane. 2023. DOI: 10.15199/33.2023.09.02.

[5] Blazy J, Drobiec Ł, Wolka P. Projektowanie fibrobetonowych posadzek przemysłowych według trzeciej i czwartej edycji Technical Report 34, w Monografie technologii betonu: XII Konferencja Dni Betonu, Wisła, 9 – 11 października 2023, ss. 1091–1104.

[6] EN 12390-5:2009. Testing hardened concrete – Part 5: Flexural strength of test specimens.

[7] JSCE-SF4. Methods of tests for flexural strength and flexural toughness of fiber reinforced concrete. 1984.

[8] Glinicki M.A. Badania właściwości fibrobetonu z makrowłóknami syntetycznymi, przeznaczonego na podłogi przemysłowe. Cement Wapno Beton. 2008; t. 13/75, nr 4: 184 – 195,.

[9] EN 14651+A1:2007. Test method for metallic fibre concrete – Measuring the flexural tensile strength (limit of proportionality (LOP), residual). 2007.

[10] RILEM TC 162-TDF. Test and design methods for steel fibre reinforced concrete, final recommendations. Materials and Structures. 2002; t. 35, nr 9: 579 – 582.

Publication supported by the Excellence Initiative – Research University program implemented at the Silesian University of Technology, 2023.

Accepted for publications: 20.11.2023 r.